

3D RECONSTRUCTION OF PHASE CONTRAST IMAGES USING FOCUS MEASURES

Vincent On¹, Atena Zahedi² and, Bir Bhanu^{1,2}

¹Dept. of Electrical and Computer Engineering, University of California, Riverside, CA 92521, USA

²Depart. of Bioengineering, University of California, Riverside, CA 92521, USA

Email: von001@ucr.edu, azahe001@ucr.edu, bhanu@cris.ucr.edu

ABSTRACT

In this paper, we present an approach for 3D phase-contrast microscopy using focus measure features. By using fluorescence data from the same location as the phase contrast data, we can train supervised regression algorithms to compute a depth map indicating the height of objects in imaged volume. From these depth maps, a 3D reconstruction of phase contrast images can be generated. This paper has shown the ability to 3D reconstruct phase contrast images using a variance metric inspired by all-in-focus methods. The proposed method has been used on A549 lung epithelial cells.

Index Terms— 3D Reconstruction, Phase Contrast Images, Focus Measures, Fluorescence, Regression

1. INTRODUCTION

Phase contrast microscopy is a contrast-enhancing optical imaging modality. It is commonly used to produce high-contrast images of specimens, such as cells, microorganisms, tissue, and other transparent objects. Phase contrast imaging has many distinct advantages over other imaging methods. Objects collected with phase contrast are more visible than traditional bright field microscopy, even displaying internal structures that were previously invisible. Additionally, living specimens do not have to be killed, fixed, or stained and can be observed during ongoing biological processes. Lastly, phase contrast is not orientation dependent like differential interference contrast (DIC) microscopy and can be imaged at angle without producing artifacts. Traditionally, phase contrast has been constrained to 2D images. However, as samples become thicker the microscope's depth-of-field is not sufficient to image the entire object [1]. Because of this, 3D image is important to fully analyze the object of interest.

3D construction can be useful for visualizing the internal compartments of cells and cell shape. Additionally, 3D phase contrast reconstruction can be used to identify individual cells in tightly packed colonies such as pluripotent stem cells, and cells which grow as tightly-packed monolayers such as lung cells. A single cell culture may contain multiple types of objects such as cell substructures, debris, media and differentiated cells. Each of these may

appear differently in an image and can greatly benefit from height and shape information provided by 3D imaging.

In this paper, we propose a novel machine learning based approach for three-dimensional rendering of cells in culture. Unlike previous methods, our method can be used with any microscopy system that has phase contrast and fluorescence. After training the machine learning algorithms, the fluorescence imaging is no longer necessary and can be used to generate 3D phase contrast volumes using only a z-stack of phase contrast images.

2. RELATED WORK AND CONTRIBUTION

Traditionally, 3D microscopy has been acquired using confocal microscopy or super-resolution microscopy because of their ability to remove out of focus light rays [2]. However, there are very few systems that provide both phase contrast and confocal/super-resolution images at the same time. Because of this we have decided to work on a system that has both phase contrast and fluorescent imaging. In fluorescent imaging, fluorescent stains are introduced to the imaging sample. By marking the contour of an object with stains, we can obtain an accurate depth ground truth.

The proposed method assumes that different parts of an object will be most in focus at different heights. Because of this, it is useful to relate our method to all-in-focus algorithms. Many of these algorithms begin by acquiring image focal stacks that are focused at different distances [3]. These methods will either use defocus or in-focus parameter to select the focal distance in which a pixel is most in focus [4]. By using an in-focus parameter, a depth map may be generated and can be used to 3D render the object of interest. In addition, these methods may be used to produce all-in-focus microscopy images. Other potential applications can include finding and maintaining autofocus during time-lapse imaging.

To the best of our knowledge 3D phase contrast has not been achieved without specialized equipment. Chen et al. [5] have produced a 3D reconstruction of polystyrene beads, however they constructed a custom LED array and axial motion stage to image the sample at different angles. The

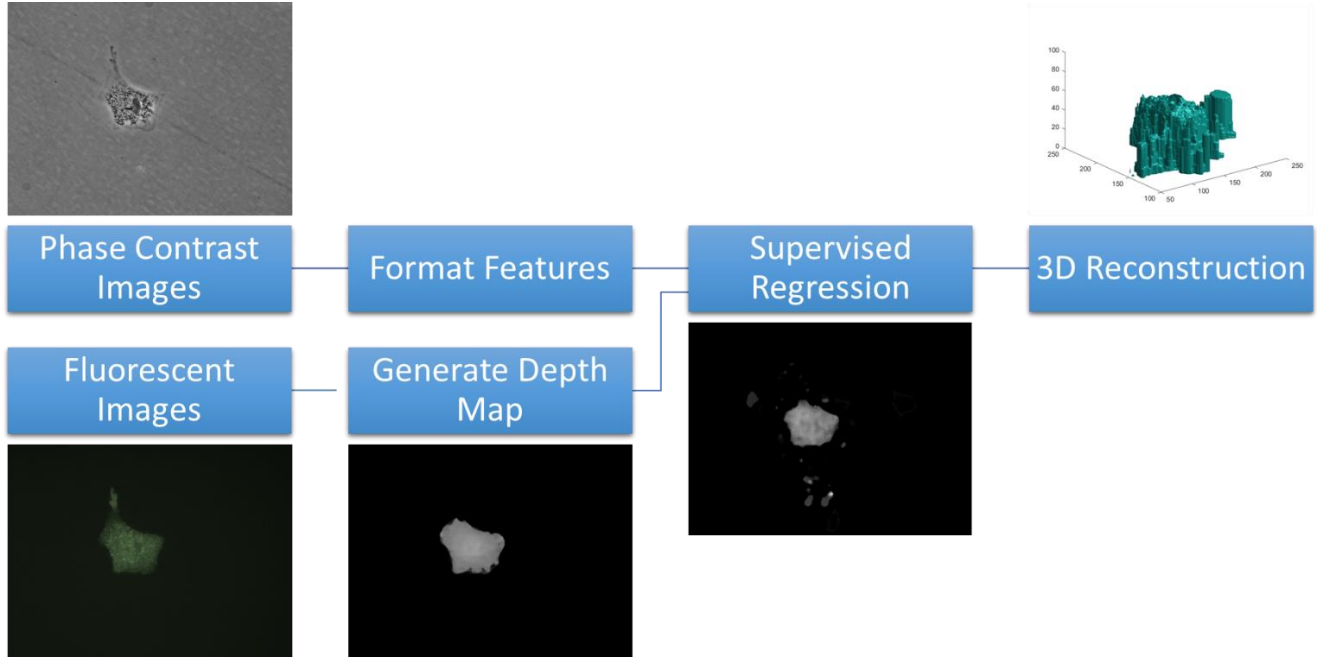


Fig. 1: System overview for phase contrast 3D Reconstruction

proposed method does not require the addition of specialized hardware to existing imaging systems.

3. THE PROPOSED METHOD

The proposed method is shown in Figure 1. The system extracts variance features from phase contrast image volumes and estimates a depth value using supervised regression. Fluorescent images are used to generate a ground truth and to provide labels to the phase contrast data. The regressed values are then reshaped into a depth map which is used for 3D reconstruction.

5.1. Ground Truth Generation

During data collection, both phase contrast and fluorescent images of size $r \times c$ were taken for various cell cultures. For each region of interest, an expert biologist focused the microscope, so that the center plane is the most in focus. From this plane, h planes above and below are collected across the z -axis of the microscope. Every plane is separated by a step size of s micrometers. In total, $H = 2h + 1$ planes are collected for each cell in each imaging modality. Each image represents a different focal distance. Phase contrast and fluorescent images collected at various heights are shown in Figure 2.

To generate a ground truth for the phase contrast 3D reconstruction, a fluorescent 3D reconstruction is generated on the same volume. Usually, these images are collected with a microscope that removes out of focused light such as

confocal or structured illumination microscopy (SIM). Since there are few systems that can collect these types of images with phase, we must compute a depth map while taking blur into account.

Our method for generating ground truth from a volume of fluorescence images is to generate a depth map representing the height of each pixel. Various in-focus measures can be used to estimate the height. Yao et al. [6] have shown that variance is a strong metric to compute an all-in-focus image. Our method begins by generating a variance volume V by convolving a variance filter through each voxel. As we are only interested in the most in-focused image, the filter is an $m \times m$ 2D filter. We have found $m=5$ to work the best empirically.

A depth map D is generated from the variance volume by the following algorithm.

1. Initialize D as a zeros matrix with the same size as the input images.
2. Loop across i and j for all pixels of D .
3. Compute the maximum value of V at (i,j) across the z -axis.
4. The value of $D(i,j)$ is the index of the maximum value across the z -axis.

As there may be some errors in the depth map, a median filter is applied to smooth the values.

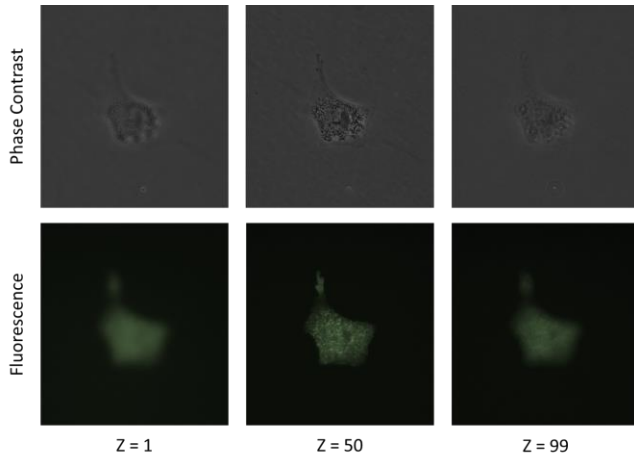


Fig. 2: Phase contrast and fluorescence images at different focal points

3.2. Input Features

Our proposed method for phase contrast 3D reconstruction is to generate a depth map based on supervised regression. To generate the features, we begin by computing a variance volume V_p using the same method to generate our ground truth. However, instead of using the fluorescence images, the phase contrast images are used. To reduce the effect of background information in our regression, we remove the background from the image before computing V_p . This is done by using the edge based segmentation method used in [7] on every image in the stack. Once objects are segmented anything below a specific size is considered a part of the background and set to zero.

After acquiring V_p , data samples are extracted by examining variance values along the z-axis. For a volume of size $r \times c \times H$, there will be $r \times c$ samples of size $H \times 1$. A label $L(i,j)$ is also assigned to each voxel based on corresponding value on the depth map $D(i,j)$.

3.3 Supervised Learning

Once extracted, the samples will be used to train a regression model. We have tested three different regression models: regression trees [8], linear support vector regression [9], least squares boosting regression [10]. Each model will take a vector of $H \times 1$ inputs and estimate a height value. After estimating a height value for the $r \times c$ samples of an image volume, these values are reshaped into a depth map D_p of size $r \times c$.

3.4 3D Reconstruction from Depth Map

Because the system is imaging only the top of cells, the method assumes that every voxel below the top voxel of the object is a part of the object. This is a safe assumption for our

data as we are analyzing in vitro cells on a dish. Once these cells attach to the substrate, the cell lay flat on the surface. Using this constraint, a labelled volume L is created from the depth map as follows:

$$L(i,j,k) = \begin{cases} 1 & \text{if } k \leq D_p(i,j) \\ 0 & \text{otherwise} \end{cases} \quad (1)$$

To reduce noise, a 2D median filter is convolved with the depth map before being used to create the labelled volume.

4. EXPERIMENTAL RESULTS

5.1. Datasets

All images have a resolution of 800x600 pixels. To reduce processing time, all images were resized to 400x300 by subsampling the pixels in the image. Phase contrast and fluorescence 3D images were acquired using the BioStation IM (Nikon Instruments, Melville NY) which is a compact cell incubator and monitoring system. 99 slices were collected at 0.3 μm spacing. A 20x objective was used to gather individual cells and small cell clusters. All images were of A549 lung epithelial cells.

A549 lung epithelial cells (human type II pulmonary alveolar adenocarcinoma cells) were obtained from (ATCC CCL-185, Manassas, VA, USA) and cultured in Ham's F-12 media supplemented with 10% fetal bovine serum (ATCC, Rockville, MD). Cells were grown until 80% confluency, at which point they were detached using 0.25% trypsin EDTA/DPBS. A549 cells were passaged every 2-3 days and medium was replenished every other day. Both cells types were grown in a 37°C incubator with 90% humidity and 5% CO₂.

In the A549s, Cyclin D1 (Red) is a marker important in cell-cycle and is localized to the nucleus. CD44 is a cancer stem cell marker, and was localized to the plasma membrane. There was an increase in the Cyclin D1 and CD44 expression on the treated A549 lung cancer cells. Acetylated α -tubulin (Green) localized to the cytoplasm.

5.2 Results

Our dataset consisted of 5 cell volumes with 400x300 data points each. A 5-fold cross-validation was performed for each regression model by training on 4 cell volumes and testing on the last volume. Figure 3 displays the depth maps of ground truth and the 3 regression models. The figure also shows the 3D reconstruction generated by the depth maps. All sub images are of the same cell.

From figure 3, the thickness of the samples is overexaggerated. Since the center plane ($z=50$) is the most in-focus plane, $z=1$ is not bottom of the cell. The $z=1$ plane is likely to be below the bottom, which explains the extra

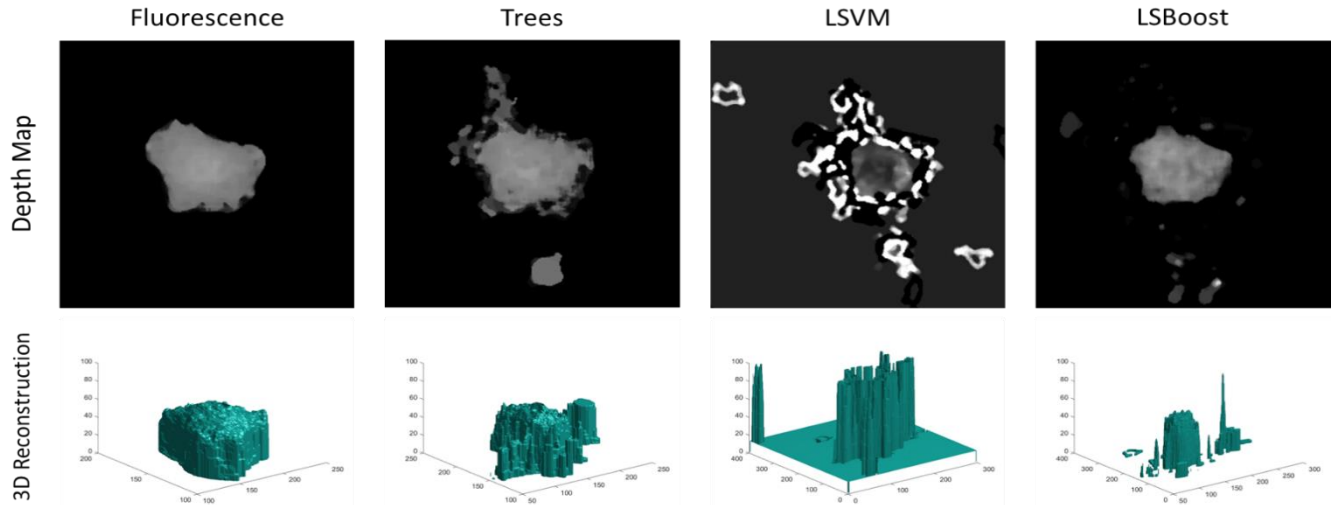


Fig. 3: Row 1: Ground truth and regression depth maps. Row 2: 3D reconstructions of volumes from depth maps

thickness seen in the 3D reconstruction. There are also errors around borders of the cell due to segmentation. As the segmentation sets the background to zero, these boundaries form an edge. These artificial edges cause an increase in the variance metric. LSVM is especially susceptible to this as seen in the extreme boundaries in the depth map.

Because the stains in the fluorescence images only target specific structures, other objects such as debris are not detected. However, they are still visible in phase contrast. One such object can be seen in the bottom of the trees depth map. These objects are then detected in the phase 3D reconstructions but not the fluorescence.

Table 1 shows the precision and recall results for each cell. Trees and LSBoost performed well on all cells except for cell 3. Cell 3 was an image stack with large dead cells which likely affected the precision results. LSVM was very sensitive to boundary conditions, causing it to perform very poorly for all cells. Figure 4 displays the $z=50$ slice of cells 2 to 5.

5. CONCLUSIONS

In this paper, we have developed a 3D reconstruction method that can be used on phase contrast images. By using

	Trees		LSVM		LSBoost	
	Precision	Recall	Precision	Recall	Precision	Recall
cell 1	72.90%	89.12%	5.95%	50.52%	85.51%	69.02%
cell 2	75.83%	56.09%	10.02%	52.09%	88.30%	47.85%
cell 3	18.68%	86.65%	3.75%	95.76%	25.57%	88.46%
cell 4	65.97%	86.00%	10.52%	45.50%	87.12%	72.15%
cell 5	62.64%	75.87%	8.75%	48.75%	75.15%	53.90%

Table 1: Depth map regression results

fluorescence data as the ground truth, the system was able to train various regression models to compute a depth map. From this depth map, a 3D reconstruction can be generated which can detect objects not shown in fluorescence. Unlike other 3D phase contrast methods, the proposed system does not require custom hardware. Also unlike other methods, our system only requires one angle to be imaged and can be used by any research group with a microscopy system capable of imaging in both phase and fluorescence.

5. ACKNOWLEDGEMENTS

The authors would to thank Dr. Prue Talbot for providing the cells and materials used in this paper. The support for this work was provided in part by NSF IGERT: Video Bioinformatics grant number DGE 0903667.

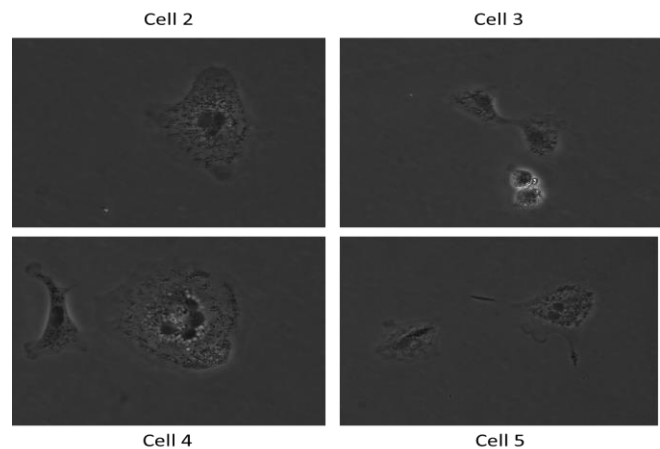


Fig. 4: Center phase contrast images of cells 2 to 5

6. REFERENCES

- [1] E. Maalouf, *Contribution to Fluorescence Microscopy, 3d Thick Samples Deconvolution and Depth-variant Psf* Maalouf. 2010.
- [2] A. Ray and A. K. Mitra, "Nanotechnology in Intracellular Trafficking, Imaging, and Delivery of Therapeutic Agents," in *Emerging Nanotechnologies for Diagnostics, Drug Delivery and Medical Devices*, Elsevier, 2017, pp. 169–188.
- [3] D. Vaquero, N. Gelfand, M. Tico, K. Pulli, and M. Turk, "Generalized autofocus," in *2011 IEEE Workshop on Applications of Computer Vision (WACV)*, 2011, pp. 511–518.
- [4] J. Koseki *et al.*, "The development of an all-in-focus algorithm for endoscopy," in *MHS2013*, 2013, no. 1, pp. 1–5.
- [5] M. Chen, L. Tian, and L. Waller, "3D differential phase contrast microscopy," *Biomed. Opt. Express*, vol. 7, no. 10, p. 3940, 2016.
- [6] Y. Yao, B. Abidi, N. Doggaz, and M. Abidi, "Evaluation of sharpness measures and search algorithms for the auto focusing of high-magnification images," 2006, vol. 6246, p. 62460G.
- [7] A. Zahedi, V. On, S. C. Lin, B. C. Bays, and E. Omaiye, "Evaluating Cell Processes , Quality , and Biomarkers in Pluripotent Stem Cells Using Video Bioinformatics," *PLOS ONE*, pp. 1–22, 2016.
- [8] W. Loh, "Regression Trees with Unbiased Variable Selection," *Korean J. Appl. Stat.*, vol. 17, no. 3, pp. 459–473, Nov. 2004.
- [9] C.-H. Ho and C.-J. Lin, "Large-scale Linear Support Vector Regression," *Jmlr*, vol. 13, pp. 3323–3348, 2012.
- [10] J. H. Friedman, "Greedy Function Approximation: A Gradient Boosting Machine," *Ann. Stat.*, vol. 29, no. 5, pp. 1189–1232, Oct. 2001.